

# TiB<sub>2</sub>-based Ceramic/1Cr18Ni9Ti Stainless Steel Composite Produced by Combustion Synthesis in Ultra-high Gravity Field

Yin Dejun, Zhao Zhongmin, Lu Xiaobo, Zheng Jian

Ordnance Engineering College, Shijiazhuang 050003, China

**Abstract:** Based on fusion bonding and atomic interdiffusion between the ceramic and stainless steel, the TiB<sub>2</sub>-based ceramic/1Cr18Ni9Ti stainless steel composite with chemical composition gradient was produced by combustion system in ultra-high gravity field (CSUGF). The presence of chemical reaction in explosive combustion and the subsequent thermal-vacuum circumstance induced by liquid products in ultra-high gravity make stainless steel partially fused, resulting in fusion bonding. XRD, FESEM and EDS results show that the interface has a good bonding, and the intermediate exhibits three dimensional network ceramic-metal graded microstructure considered as a result of intensive interdiffusion of atoms. Vickers hardness profile reveals the quasi-parabola relationship of the hardness to the testing distance from the ceramic matrix to the steel substrate. Meanwhile, interfacial shear fracture of the composite presents the mixed mode consisting of intercrystalline fracture along TiB<sub>2</sub> platelets and ductile fracture in Fe-Ni-Cr alloy, presenting interfacial shear strength (325 ± 25) MPa.

**Key words:** combustion synthesis in ultra-high gravity field (CSUGF); microstructure; hardness; shear strength

Functionally graded materials (FGMs) have emerged as an important class of materials for structural, wear, transportation and electrical applications, primarily as a result of their ability to exhibit superior strength-to-weight and strength-to-cost when compared to equivalent monolithic commercial alloys<sup>[1-3]</sup>. At present, FGM bulks, joints and coatings can be manufactured by various processes like spark plasma sintering (SPS)<sup>[4]</sup>, plasma transferred arc (PTA)<sup>[5]</sup>, transient liquid phase bonding (TLPB)<sup>[6]</sup>, laser cladding (LC)<sup>[7]</sup>, and chemical vapor deposition (CVD)<sup>[8]</sup>. Meanwhile, the processes of FGM coating in the industrial scale have reached a considerable level of maturity. However, because of the limits by powder forming process and heavy precision equipment, the routes of large-scale FGM bulks and joints are still at the developing stage. Hence, it has become an important issue of FGM development in the world to actively develop a series of low-energy-consumption, low-cost and rapid-production-flow routes along with the novel process assisted with external field for preparing FGM bulks<sup>[4,9-12]</sup>.

The combustion synthesis in ultra-high gravity field (CSUGF) technique has been a novel and economical method which emerged in recent years, and will be used widely due to its ability to fabricate ceramic bulks with compact microstructure, high hardness and low porosity<sup>[13]</sup>. But there are few reports on FGM bulks and joints using CSUGF method. The objective of the present work is to explore the fabrication of TiB<sub>2</sub>-based ceramic/1Cr18Ni9Ti stainless steel composite by CSUGF. The phase constituents, microstructure, hardness and shear strength of the composite with graded interfacial microstructure were investigated.

## 1 Experiment

Raw materials purity (>97%) B<sub>4</sub>C powder with particle size <3.5 μm and high purity (>99%) Ti powder with particle size <50 μm were used. The molar ratio of Ti to B<sub>4</sub>C in reaction system is shown in Eq.(1).

Received date: August 25, 2016

Foundation item: National Natural Science Foundation of China (51072229)

Corresponding author: Zhao Zhongmin, Ph. D., Professor, Teaching and Research Section of Mechanical Manufacturing, Department of Vehicle and Electric Engineering, Ordnance Engineering College, Shijiazhuang 050003, P. R. China, Tel: 0086-311-87994737, E-mail: 2544219238@qq.com

Copyright © 2017, Northwest Institute for Nonferrous Metal Research. Published by Elsevier BV. All rights reserved.



After blending and mechanically activating the above powders in a ball milling machine for 2 h, the powder blends were pressed to be the powder compacts. Subsequently, 1Cr18Ni9Ti stainless steel with 100 mm in diameter and 6 mm in thickness was put at the bottom of the crucibles, followed by filling the powder compacts in the crucible. The chemical composition of 1Cr18Ni9Ti is 70.015Fe-0.12C-1.0Si-2.0Mn-18.0Cr-8.0Ni-0.8Ti-0.03S-0.035P (wt%). The crucibles were fixed in the centrifugal machine system, and then, the centrifugal machine started to increase the acceleration of crucible to be about 2000 g ( $1 \text{ g} = 9.8 \text{ m/s}^2$ ). As the top of the reaction system was ignited to start thermal explosion reaction in ultra-high gravity field, the centrifugal machine continued to run for 1 min. As the crucibles were cooled to the ambient temperature, the centrifugal machine was stopped and the graphite crucibles were taken out of the combustion chambers. Finally, the hexagonal product of the composite was obtained after the samples were worked by electric discharge machining, as shown in Fig.1.

The phase identification was applied by X-ray diffraction (XRD). The microstructure was observed by field emission scanning electron microscopy (FESEM) equipped with EDS. The indentation test was conducted for a loading time of 15 s and a load scale of 196 N to measure the hardness by Vickers hardness tester. Meanwhile, the composite was cut and ground into ten rectangular bars measuring 20 mm (length)  $\times$  20 mm (width)  $\times$  10 mm (height) for determining the interfacial shear strength of ceramic-metal joints.

## 2 Results and Discussion

After cutting the sample into the several pieces at interval 0.5 mm from the ceramic matrix to steel substrate, the XRD patterns of the composite are shown in Fig.2. It can be seen that the intermediate mainly consists of  $\text{TiB}_2$  primary phases, non-stoichiometric TiC as well as Fe-Ni-Cr and this ensures the completion of the reaction and absence of any secondary reaction. Meanwhile, with increasing the distance from the ceramic matrix to steel substrate, the diffraction peaks of  $\text{TiB}_2$  and TiC drop sharply, whereas Fe-Ni-Cr peaks rise rapidly. It indicates that with the increasing distance in the intermediate from the ceramic matrix to steel substrate, volume fraction of  $\text{TiB}_2$  and TiC decreases while Fe-Ni-Cr increases reversely. The formation of metal matrix composite with graded interfacial microstructure is confirmed from the X-ray diffraction analysis.

It can be seen that the interface has a compact microstructure, good bonding and no obvious cracks, as shown in Fig.3a. Fig.3b shows that the very thin band

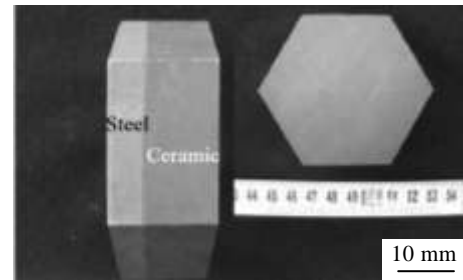


Fig.1 Hexagonal brick of the  $\text{TiB}_2$ -based ceramic/1Cr18Ni9Ti stainless steel composite

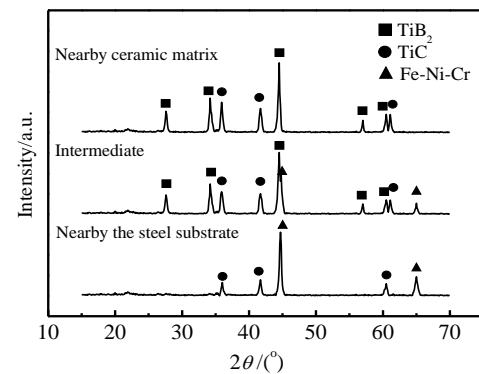


Fig.2 XRD patterns of different areas from the ceramic matrix to steel

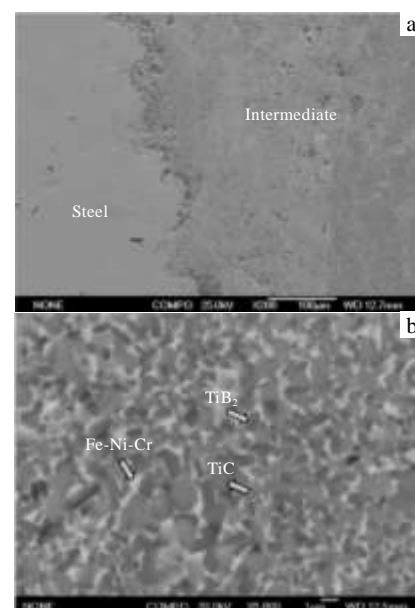


Fig.3 FESEM images of the intermediate between the ceramic and steel: (a) low-magnification and (b) high-magnification

of Fe-Ni-Cr is formed to surround the  $\text{TiB}_2$  and TiC with the average diameter less than 1  $\mu\text{m}$  in the intermediate. Hence, the thermal explosion mode caused by the introduction of ultra-high gravity field promotes liquid fusion, atomic interdiffusion and subsequent Fe-Ni-Cr liquid flow; then, three dimensional network ceramic-metal graded microstructure comes into existence between the ceramic matrix and steel substrate which produce a considerable increase in toughness.

In terms of the Ref.[14-16], the introduction of ultra-high gravity field increases the energy-release rate of chemical reaction, and combustion rate is increased rapidly so that the combustion characterization in high-gravity field is similar to thermal explosion, resulting in not only rapid escape of the gas in reactive blend during combustion reaction but also the formation of thermal vacuum circumstances around the products. As a result, high-temperature liquid products consisting of  $\text{TiB}_2$  and TiC liquids are achieved rapidly, and the surface of stainless steel is also molten. Subsequently, intensive liquid fusion and atomic interdiffusion happen between the liquid ceramic and the molten steel, resulting in the formation of the liquid intermediate from the ceramic to the steel substrate. However, because of high melting entropy and high atomic concentration of Ti and B in liquid ceramic,  $\text{TiB}_2$  as the leading phase firstly nucleates and grows from the liquid ceramic nearby the intermediate, followed by the nucleation and growth of TiC. Subsequently, Fe-Ni-Cr liquid is extruded by the growing  $\text{TiB}_2$  and TiC solids, and constantly flows toward the steel substrate; thus, thin Fe-Ni-Cr liquid remains to surround the developed  $\text{TiB}_2$  and TiC solids in the intermediate nearby the solidified ceramic, whereas the irregular coarsened Fe-Ni-Cr liquid has to stay at the intermediate away from the solidified ceramic. After the solidification of liquid intermediate, very thin band of Fe-Ni-Cr is formed to surround the ceramic phases of  $\text{TiB}_2$  and TiC in the intermediate nearby the ceramic, whereas the coarse irregular particles of Fe-Ni-Cr either alone exist or surround the  $\text{TiB}_2$  (or TiC)-enriched regions in the intermediate away from the ceramic. Meanwhile, because of high diffusion rate of C relative to B atoms, C atoms spread away from the liquid ceramic farther than B atoms do, and there are yet some C atoms in the intermediate nearby the steel substrate even if there is absence of B atoms. As a result, there are a number of sub-micrometer or micro-nanometer particles of non-stoichiometric  $\text{TiC}_{1-x}$  embedded in the intermediate. Hence, three dimensional network spatial-span-scale (i.e.  $\text{TiB}_2$  and TiC phases transform sub-micrometer even micro-nanometer scale from the micrometer one) graded microstructure comes into existence between the ceramic and stainless steel substrate through liquid fusion, atomic interdiffusion and subsequent Fe-Ni-Cr liquid flow.

Fig.4 shows the curves of Vickers hardness profile from

the ceramic to steel substrate. It can be seen that the change in hardness distribution between the ceramic and steel substrate presents the quasi-parabola relationship of the hardness to the testing distance from the ceramic to the steel substrate. Meanwhile, the interfacial shear strength of the metal matrix composite is measured as  $(325 \pm 25)$  MPa.

FESEM images of Fig.5 show that shear fracture surface of the interfaces presents a rough and uneven shape. Interfacial shear fracture not only takes place at the ceramic nearby the intermediate, presenting the traces of partially-bared  $\text{TiB}_2$  platelets and the grooves resulting from pull-out and break-down of small-size  $\text{TiB}_2$  platelets, as shown in Fig.5a, but also happens in the intermediate, presenting large-scale ductile fracture due to the plastic deformation of Fe-Ni-Cr alloy, as shown in Fig.5b. Hence,

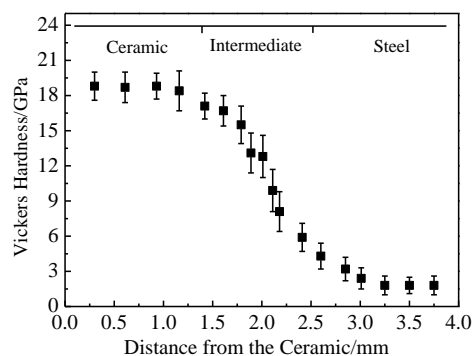


Fig.4 Vickers hardness profile of the composite from the ceramic to steel substrate

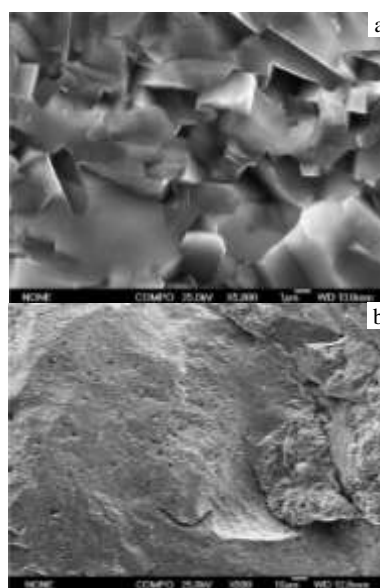


Fig.5 FESEM morphologies of interfacial shear fracture of the composite: (a) the ceramic nearby the intermediate and (b) the intermediate

it is considered that interfacial shear fracture exhibits the mixed mode of intercrystalline fracture along fine  $\text{TiB}_2$  platelets and ductile fracture in Fe-Ni-Cr due to the presence of three dimensional network ceramic-metal graded microstructure between the ceramic and the steel.

### 3 Conclusions

1) By taking stainless steel as the substrate, the  $\text{TiB}_2$ -based ceramic/1Cr18Ni9Ti stainless steel composite with graded microstructure is prepared by reaction fusion and liquid diffusion during combustion system in ultra-high gravity field (CSUGF).

2) The intermediate of the composite is composed of  $\text{TiB}_2$ , TiC and Fe-Ni-Cr. The interface has a good bonding with no obvious cracks and the intermediate exhibits three dimensional network ceramic-metal graded microstructure.

3) Vickers hardness profile reveals the quasi-parabola relationship of the hardness to the testing distance from  $\text{TiB}_2$  based ceramic to the stainless steel, and interfacial shear strength reaches  $(325 \pm 25)$  MPa. The shear fracture mode of the composite is the mixed shear fracture mode of intercrystalline fracture along fine  $\text{TiB}_2$  platelets and ductile fracture in Fe-Ni-Cr.

### References

- Suresh S, Shenbag N, Moorthi V. *Procedia Engineering*[J], 2012, 38: 89
- Zhang J, Zhang D Q, Wu P W et al. *Rare Metal Materials and Engineering*[J], 2014, 43(1): 47
- Tang Y W, Chen F, Cao Z Q et al. *Rare Metal Materials and Engineering*[J], 2014, 43(1): 194 (in Chinese)
- Kwon H, Leparoux M, Kawasaki A. *Journal of Materials Science and Technology*[J], 2014, 30(8): 736
- Darabara M, Bourithis L, Diplas S et al. *Applied Surface Science*[J], 2008, 254(13): 4144
- Zhang G F, Zhang J X, Pei Y et al. *Materials Science and Engineering A*[J], 2008, 488(1-2): 146
- Li J N, Chen C Z, He Q S. *Materials Chemistry and Physics* [J], 2012, 113: 741
- Shimada S, Fuji Y, Tsujino J et al. *Surface and Coatings Technology*[J], 2010, 204(11): 1715
- Jia D C, Zhou L Z, Yang Z H et al. *Journal of the American Ceramic Society*[J], 2011, 94(10): 3552
- Yin C, Zhong S M, Chen W F. *Communications in Nonlinear Science and Numerical Simulation*[J], 2012, 17(1): 356
- Yin C, Chen Y Q, Zhong S M. *Automatica*[J], 2014, 50(12): 3173
- Xi W J, Peng R L, Wu W et al. *Journal of Materials Science* [J], 2012, 47(8): 3585
- Liu G H, Li J T. *Journal of Asian Ceramic Societies*[J], 2013, 1(2): 134
- Zhao Z M, Zhang L, Song Y G et al. *Scripta Materialia*[J], 2009, 61(3): 281
- Wang L L, Munir Z A, Maximov Y M. *Journal of Materials Science*[J], 1993, 28(14): 3693
- Huang X G, Zhao Z M, Zhang L. *Materials Science and Engineering A*[J], 2013, 564: 400

## 超高重力场燃烧合成 $\text{TiB}_2$ 基陶瓷/1Cr18Ni9Ti 不锈钢复合材料

尹德军, 赵忠民, 路晓波, 郑 坚

(军械工程学院, 河北 石家庄 050003)

**摘要:** 采用超高重力场燃烧合成技术, 通过陶瓷和不锈钢之间的熔化连接与原子互扩散, 制备出界面具有化学成分梯度特征的 $\text{TiB}_2$ 基陶瓷/1Cr18Ni9Ti不锈钢复合材料。因超高重力场燃烧合成工艺具有“爆燃”的特性以及超高重力场所形成的高温真空环境, 使得不锈钢表面发生部分熔化, 进而实现了陶瓷/不锈钢的熔化连接。经XRD、FESEM及EDS分析发现, 接头界面连接良好, 并因原子的强烈互扩散在界面过渡区形成了三维网络陶瓷/金属梯度复合结构。经测试发现, 维氏硬度值与陶瓷基体至不锈钢基底测试距离的关系曲线呈近似抛物特征。同时, 复合材料的界面抗剪切强度达到 $(325 \pm 25)$  MPa, 其界面断裂模式是由 $\text{TiB}_2$ 片晶沿晶断裂和Fe-Ni-Cr合金相延性断裂的混合模式组成。

**关键词:** 超高重力场燃烧合成 (CSUGF); 显微组织; 硬度; 剪切强度

作者简介: 尹德军, 男, 1990年生, 硕士, 军械工程学院, 河北 石家庄 050003, 电话: 0311-87994737, E-mail: 1051994475@qq.com